Hindawi Publishing Corporation
EURASIP Journal on Wireless Communications and Networking
Volume 2008, Article ID 734216, 7 pages
doi:10.1155/2008/734216

Research Article

A Study of Gas and Rain Propagation Effects at 48 GHz for HAP Scenarios

S. Zvanovec, P. Piksa, M. Mazanek, and P. Pechac

Department of Electromagnetic Field, Faculty of Electrical Engineering, Czech Technical University in Prague, Technicka 2, 166 27 Prague 6, Czech Republic

Correspondence should be addressed to S. Zvanovec, xzvanove@fel.cvut.cz

Received 31 October 2007; Accepted 18 March 2008

Recommended by Marina Mondin

The atmosphere and rainfall significantly limit the performance of millimeter wave links and this has to be taken into account, particularly, during planning of high altitude platform (HAP) networks. This paper presents results from the measurement and simulation of these phenomena. A simulation tool from our previous analyses of terrestrial point-to-multipoint systems has been modified for HAP systems. Based on a rainfall radar database and gas attenuation characteristics as measured by a Fabry-Perot resonator, the performance of a simple link, two-branch diversity links, and more complicated HAP scenarios are discussed.

1. INTRODUCTION

Several features in the atmosphere greatly limit system performance in the millimeter-wave band. This is true mainly for HAP systems working at a frequency of 48 GHz. Rain drops and atmospheric gas influence the propagation of electromagnetic waves in many ways, causing an undesirable decrease in the system's service availability.

The work presented here is partly based on our previous research, which was focused on terrestrial point-to-multipoint systems [1], where a terrestrial point-to-multipoint system outage improvement probability was derived as a function of rainfall and system parameters. A new method was proposed to classify the spatial properties of a rain event. The aim is to validate the applicability of the approach to HAP scenarios, where route diversity is applied. Rather than generating diversity gain statistics, system performance during a rain event is simulated in both time and space.

In order to support system performance analyses with appropriate input parameters, a gas attenuation measurement and a rainfall radar database are utilized.

The paper is organized along the following pattern. In the first part of the paper, the gas attenuation aspects are discussed. Measurement and simulation results together with an enhancement of the Fabry-Perot resonator measurement technique are then introduced. The next section deals with the utilization of rainfall radar data during simulations of HAP systems. The following part reveals simulation results for a single link, two-branch diversity links, and a HAP system network, when the gas attenuation and the rainfall radar database are introduced. The paper concludes with a brief summary.

2. GAS ATTENUATION MEASUREMENTS

The atmosphere limits the performance of millimeter-wave systems. Many papers introducing gaseous attenuation measurements can be found in the literature (e.g., [2–4]). Most of the measurements performed to date are based on the radiometric approach, which uses a radiometer pointed at a satellite. Together with the attenuation, additional atmospheric properties such as temperature, pressure, and gas composition and humidity are collected. The attenuation introduced by atmospheric gases can either be described using an accurate physical model, such as Liebe's model [5] for frequencies ranging from 1 GHz up to 1 THz, or it can be approximated by probabilistic models such as the ITU-R P. 676 [6] or Salonen's models [7]. The ITU-R P.676 includes two models for the calculation of gaseous attenuation:

(i) a complete line-by-line method, which sums the contributions from 44 oxygen lines and 30 water-vapor lines below 1000 GHz,

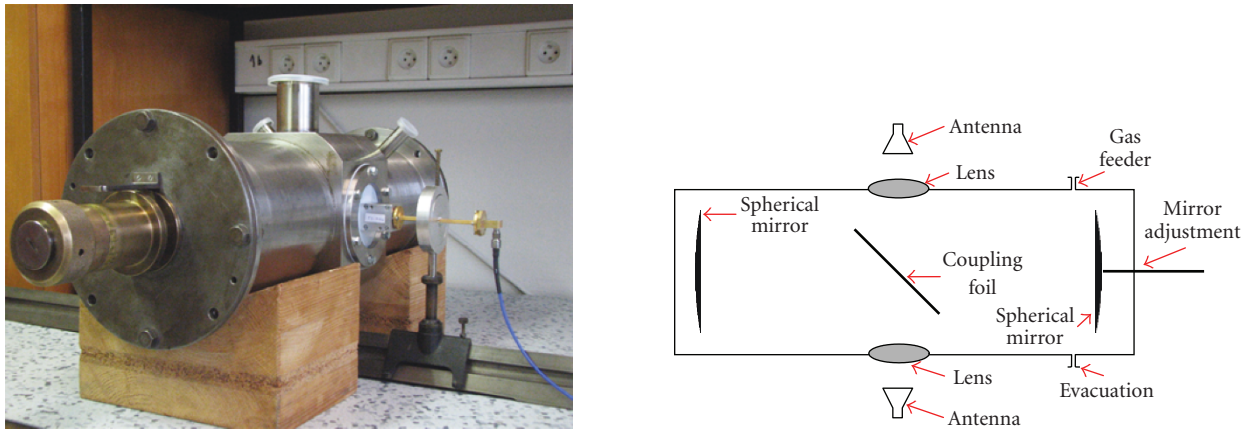

(a) (b)

Figure 1: Fabry-Perot resonator for gas attenuation measurements: (a) equipment, (b) schematic.

(ii) simplified algorithms based on a curve-fitting to the line-by-line calculation.

Nevertheless, in the HAP scenario, several different situations can be observed from the gas attenuation point of view. Atmospheric properties are different for inter HAP connections when compared to the classical HAP to ground user links. A support measurement system is advisable for a proper investigation of atmospheric attenuation.

The main aim of this section is to introduce a measurement system with the Fabry-Perot resonator (see Figure 1) and to discuss the results of both simulations and laboratory measurements of gas attenuation. The equipment itself was designed at the Czech Technical University in Prague . Several aspects of the experiments described below supplement the millimeter-wave high resolution spectroscopy measurement campaign [8], which has been accomplished in cooperation with the Institute of Chemical Technology in Prague.

2.1. Enhancements of the measurement technique

The principal virtue of laboratory measurements of atmospheric gases lies in the possibility of adjusting the gas medium in terms of the homogeneity of a particular gas composition, and in terms of the proper distribution, temperature, and pressure, a situation which can never be truly achieved in the case of open range measurements. Spectroscopy cavities, Fabry-Perot resonators [9], or very long tubes introducing extremely precise tools compared to the statistically-based measurements in open areas, where the variability of the atmosphere cannot be adequately defined.

A Fabry-Perot resonator (Figure 1(a)) working from 18 GHz up to hundreds of GHz was developed for the gas attenuation measurements. The main layout of the resonator is depicted in Figure 1(b). It comprises a tube-shaped cavity, two spherical mirrors positioned to set particular resonances, and a dielectric foil placed inside a cavity. One mirror is placed in a fixed position, while a second mirror can be adjusted in 1 μm steps. The foil accomplishes the transition of electromagnetic waves via dielectric lenses into and from the perpendicularly placed feeders.

The sensitivity of the Fabry-Perot resonant cavity is the result of its very high-quality factor. In this case, the absorption measurement is based on the measurement and consequential evaluation of the quality factor of the empty and gas-filled resonator.

The Fabry-Perot resonator was simulated via the FEKO electromagnetic simulator [10] using a method of moments in frequency domain with approximations of the multilevel fast multipole method (MLFMM) on metallic mirrors and the uniform theory of diffraction (UTD) on dielectric foil. The simulated resonator deployment can be seen in Figure 2(a). In order to simplify the simulations, only mirrors (shown squared in the direction of the x-axis) and a coupling foil were considered. The electromagnetic field is fed toward the z-axis (in a downwards direction).

The data of the near field obtained from the simulation were thereafter analysed in Matlab. The main objective was to obtain a frequency dependence of the transferred power. Based on these simulations, the parameters of the resonator were derived in order to reach the highest possible quality factor values. Performance of the Fabry-Perot resonator in terms of the radiation pattern (i.e., scattering of energy from the center of the coupling foil in specific directions), as simulated in FEKO, is depicted in Figures 2(b) and 2(c). In the case of an arbitrary nonresonant frequency (see Figure 2(b)), almost all energy is transmitted through the resonator. On the contrary, during the resonance (Figure 2(c)), in this particular graph at the frequency of 30 GHz, part of energy is absorbed into the resonator, and part is reflected back to the transmitter.

Losses observed in the Fabry-Perot resonator comprise the measured attenuation of an inserted medium, an additional undesirable diffraction, reflection losses at the mirrors, and coupling loss due to the dielectric foil. To properly design the measurement equipment, these additional frequency dependent losses have to be eliminated as much as possible. The first of the losses, the reflection loss, was decreased during system tuning by the $5 \cdot 10^{-5}$ m thick golden layer on the mirrors, which fully met the required depth of penetration for the gold of $0.59 \cdot 10^{-6}$ m at the lowest working

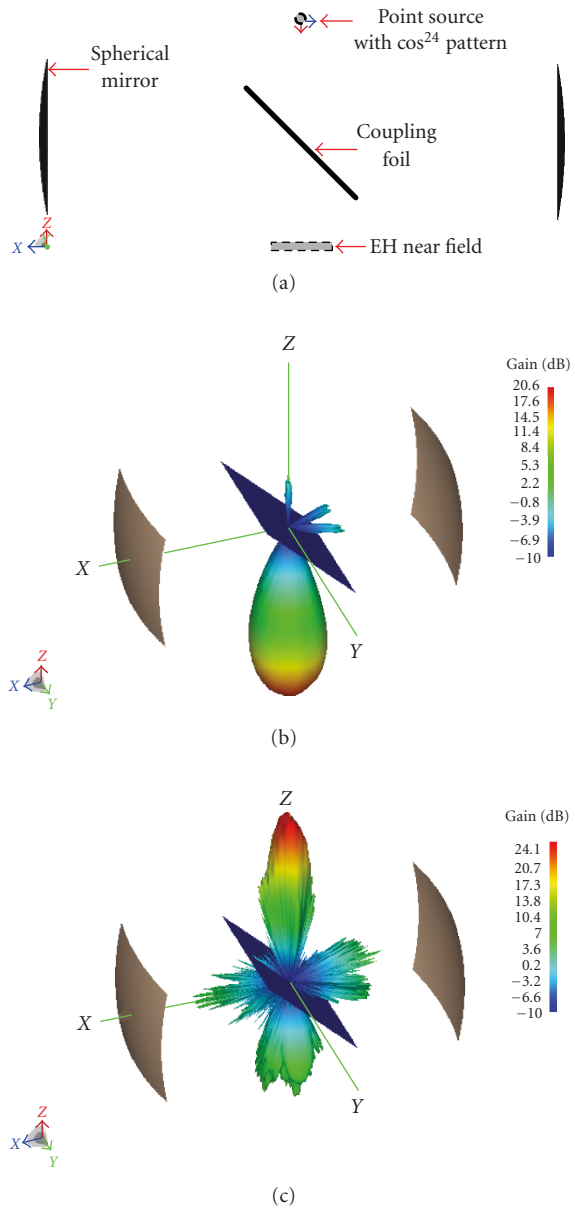

Figure 2: Performance of the Fabry-Perot resonator: (a) configuration, (b) results in terms of the radiation pattern as simulated in FEKO for the nonresonant frequency, (c) as simulated for the resonant frequency.

frequency of the resonator (18 GHz). The diffraction loss, introducing a spilling over of electromagnetic wave at the mirrors, was accompanied by a proper relation between the distance and curvature of the mirrors. A stainless steel tube-shaped cavity with a length of 0.555 m and diameter of 0.189 m, and two positioned spherical mirrors with 0.455 m radius of curvature were utilized. The confocal deployment of mirrors was chosen in order to meet a stability criterion for the Fabry-Perot resonator. The last negative loss, introduced by the coupling loss, was found to be dependent on the thickness and material parameters of the dielectric coupling foil. A 0.1 mm thick dielectric polythene coupling foil (see in Figure 2(a)) was inserted inside the resonator cavity in order

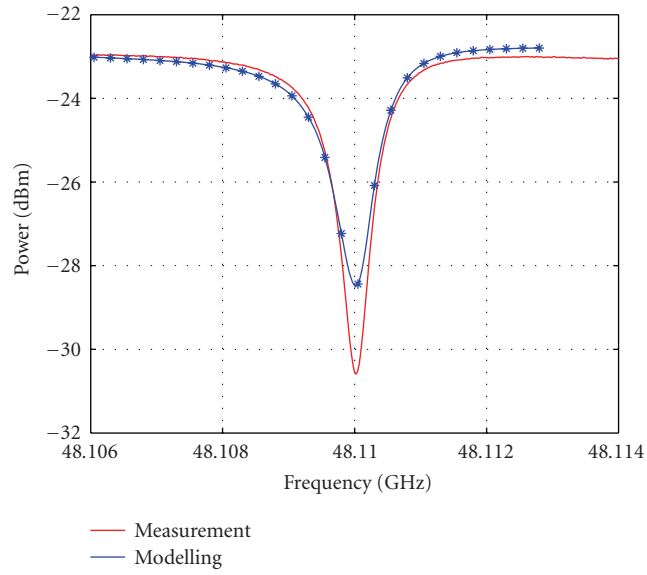

Figure 3: Comparison of measured and simulated received signal levels at a resonant frequency of 48 GHz.

to accomplish the transition of electromagnetic waves into and from the perpendicularly placed feeders.

It should be emphasized that the developed Fabry-Perot resonator is suitable for a frequency range from 18 GHz (lower frequencies are limited by diffraction losses at the mirrors) to 400 GHz, where coupling losses at the dielectric foil predominate.

Energy is led into and out of the resonator via dielectric lenses (placed in the two opposite side windows of the resonator; one of these windows can be seen in Figure 1), whose parameters had to be derived using CST microwave studio [11] simulations. It has to be emphasized that this software was used because a horn antenna and dielectric lens can be simulated more effectively in CST in the time domain (only a single simulation needed for the broadband response) than in FEKO in the frequency domain (above discussed simulations). The main demands were to ensure the best Gaussian distribution of the electromagnetic field coupling into the resonator, to keep a uniform waveform inside the resonator, and to avoid saturation of the measured gas due to the improper focusing of the energy. The optimal field distribution on the coupling foil and the position of the feeding antenna in front of the lens were also optimized (in accordance with [12]). Teflon (PTFE) with $\varepsilon_r = 2.02$ and $tg\delta = 0.003$ was utilized for the lenses. The optimal lens shape, having a spherical inner surface and an elliptical outer surface, was derived.

2.2. Gas attenuation measurement results

Measurements of the gas attenuation were accomplished with the Fabry-Perot resonator. The comparison of the measured and simulated received signal levels of Fabry-Perot resonator filled with standard laboratory air at the resonant frequency of 48 GHz is shown in Figure 3. Although both the measured and the simulated resonance have similar

shape and the same resonant frequency, an undesired slight difference in the peaks at the resonant frequency can be observed in the graph. It is caused by the fact that it was impossible to get exact properties of the air medium for the simulation tool in this test measurement.

A comparison of measured gas attenuation and the attenuation derived by ITU-R P.676 [6] for the standard atmosphere at a temperature of 293.15 K, a pressure of 1013 MPa, and a water vapor density of 7.5 g/m^3 is depicted in Figure 4. In this case, the gas attenuation was measured in the frequency range from 47.9 GHz to the 48.2 GHz assigned for HAP downlink connections (ITU-R F.1550 [13]). Differences between the measured and calculated values can be caused by additional gas molecules in the measured gas medium, which are not considered in ITU (it comprises oxygen and water-vapor lines only). For example, the resonance of an asymmetric molecule of H_2S can be observed near the frequency 48 GHz [14].

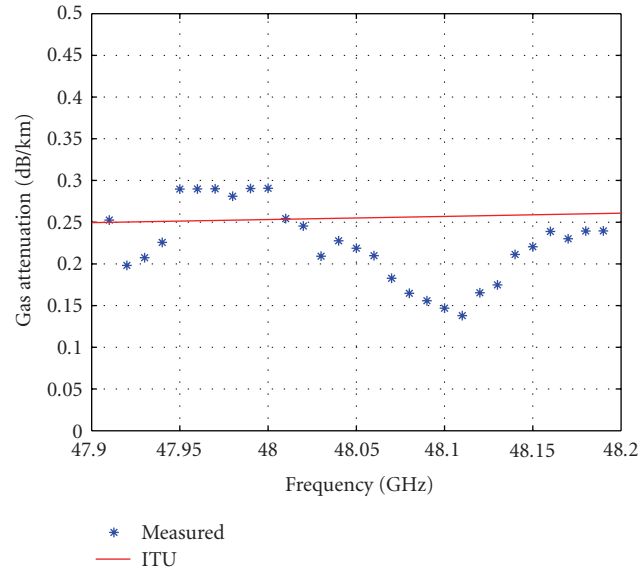

Figure 4: Comparison of the measured gas attenuation to [6].

3. RAINFALL RADAR DATA

Rain events can affect the propagation of electromagnetic waves in the millimeter wave band much more significantly than gas attenuation. For a proper assessment of the rain's influence, it is crucial not to limit oneself only to statistics valid for a single earth station to HAP link. Time and spatial dependences should also be taken into account. Rainfall radar data for a given region [15] were used as input for the simulations. Data were taken from a modern weather radar network (CZRAD) consisting of two state-of-the-art Doppler C-band weather radars, which cover the entire area of the Czech Republic with volume scans of up to 256 km in range [16]. The principle of Doppler radars is based on the transmission of electromagnetic energy into the atmosphere (hundreds of pulses per second) and the reception of backscattered energy. Doppler radars provide measurements not only of the radar reflectivity but also of the frequency change of the backscattered signal, which can be used to determine the radial velocity of atmospheric precipitation. For specific purpose, radar images with dimensions of 50 × 50 km, a 1 km grid, and 1-minute time steps were generated. Areas of up to 150 × 150 km can be analyzed from these rainfall radar scans.

A rain event database containing over 1.5 million radar images for the Czech Republic for the period from 2002–2004 was created for the simulations [1]. One of the rain scans from the middle of the rain event in 2003 is depicted in Figure 5. Three significant intensive rain cells with rain rates higher than 60 mm/hour were observed.

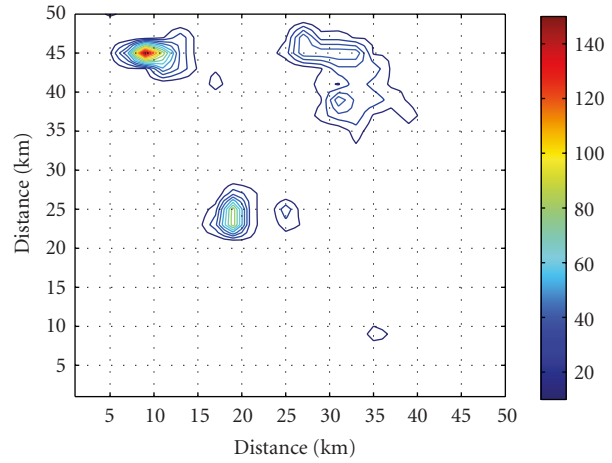

Figure 5: Rain distribution (contours) in mm/hour during a rain event.

4. HAP PERFORMANCE SIMULATION

In order to fully analyze propagation issues for HAP systems at the frequency of 48 GHz, a propagation simulation tool was developed. The core of the tool was incorporated from our previous work [1] dealing with terrestrial point-to-multipoint networks. Several modifications had to be made in order to adapt the computation models to HAP scenarios. The possibility of specifying the positions and distributions of both ground users and HAP stations, respectively, can be emphasized as the main feature from a scenario deployment point of view. This tool includes the essential parameters for investigation of wave propagation in the millimeter-wave band:

(i) rain characteristics—either statistically described parameters based on [17] or the above-mentioned rainfall radar data,

(ii) gas attenuation—this measurement was discussed in the previous section.

Based on input parameters, several HAP propagation features, ranging from simple link statistics up to complex HAP network performance, can be analyzed. Results from propagation analyses will be discussed in the following sections.

4.1. Single link and two diversity links deployment

Single HAP to a ground user link suffers from temporal rain attenuation. To combat this phenomenon, suitable rain fade margins are set during an assessment of the link budget or fade mitigation techniques, like power control and adaptive coding, are implemented [18]. Nevertheless, this solution is not always possible, particularly, for services requiring high availability. The cumulative distribution function of rain attenuation as analyzed for a 10 km (ground distance) link from the user to the HAP, which was set in the attitude of 20 km, is depicted in Figure 6. The curve is valid for the annual rain evolution over Prague, Czech Republic, in 2002.

An outage of a connection to the main HAP can be mitigated if users affected by the rain could reconnect to another station using route diversity (the principal scenario of route diversity can be seen in Figure 7). This is especially true for distant users, whose links to the main HAP could lead through a rainy area, even though these particular users are not themselves experiencing the rain event. The improvement in performance in dB between the single link attenuation and the joint two links attenuation at a given probability level is often referred as the diversity gain. The improved availability of particular user when route diversity is utilized can be evaluated or measured by the joint attenuation statistics. Many researches in a similar field have already been carried out dealing with earth-space diversity [19] and with diversity for terrestrial point-to-multipoint systems (e.g., [20, 21]). In [22], a method to establish the joint site attenuation statistics for a HAP station connected with two earth stations was developed based on combinations of satellite earth and terrestrial approaches. An analysis of the proper deployment of two diversity terminals received from a single HAP station was presented. The optimal diversity user separation has been found to be 10 to 20 km, providing 99.9% availability. A similar approach (although more in-depth), which considered correlations of rain attenuation distributions, was derived in [23].

The comparison of complementary cumulative distribution functions of rain attenuation for the above-discussed single HAP to user link at 48 GHz and, newly, for two-branch diversity links, where a user is able to connect to two HAPs, can be seen in Figure 6 In the latter case, one of the two diversity links was identical ($d_{\text{main}} = d_{\text{diversity}}$) to the standalone link and the second was angularly separated by $\varphi = 120^{\circ}$; both links had land distance of 10 km.

The diversity gain is expressed in Table 1. It can be clearly seen that a diversity gain of 1.5 dB for 99.9% availability can be achieved using route diversity. The diversity gain has a tendency to increase with the required availabilities (e.g., 7.1 dB for 99.99%).

The graph we referred to above only gives an illustrative example of the application of route diversity. The diversity gain is dependent on link length ratios, angular separations, and availabilities.

4.2. Utilization of route diversity in HAP systems

A more sophisticated approach involves an analysis of the whole system within a given area. The performance of the HAP system can be assessed in terms of outage probability in relation to the total number of operated links. The case discussed above, with two joined links, is now spread over a particular area based on the assumption that each user has the possibility of choosing another HAP station in the event of a link outage due to rain attenuation. In this way, HAP system performance can be studied simultaneously. In [24], different system outages during two storms with similar characteristics common for single links, but with different spatial features were analyzed.

To analyze system performance, an outage improvement probability $P(\%)$—a parameter taken from terrestrial point-to-multipoint system analyses [1]—was utilized. The outage

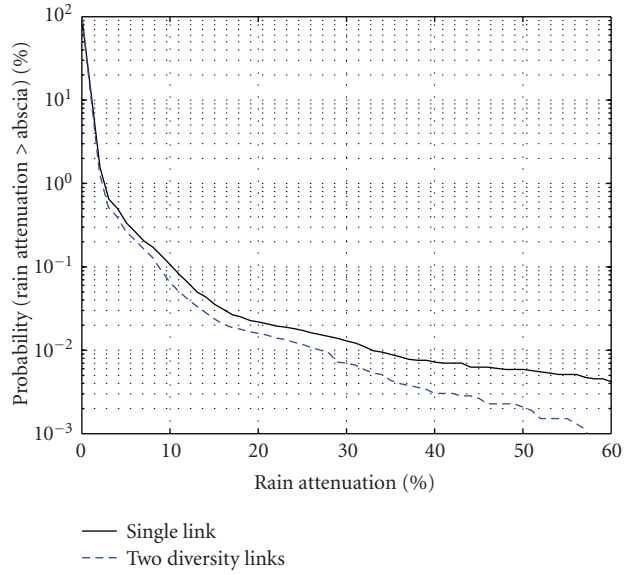

Figure 6: CDFs of rain attenuation for a single link and two-branch diversity links with the angular separation of 120 degrees and a ground link distance is 10 km.

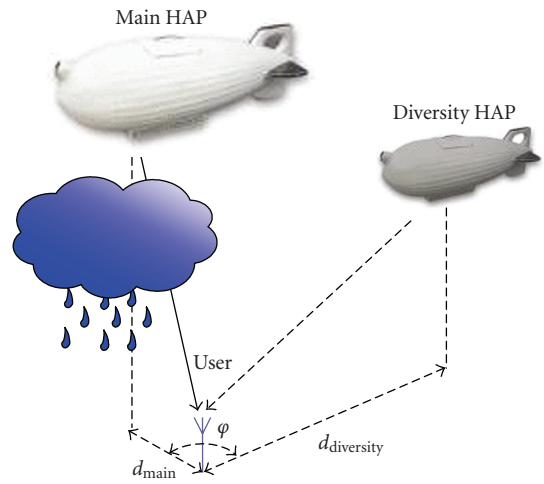

Figure 7: Basic scenario of the route diversity.

Table 1: Diversity gain of two diversity links with an angular separation of 120 degrees and a ground link distance of 10 km.

Availability (%)	Diversity gain (dB)
99.000	0.4
99.900	1.5
99.950	2.0
99.970	2.5
99.990	7.1
99.995	20.5
99.997	27.9
99.999	34.4

improvement probability is defined as the percentage of users with a successfully established diversity link out of the total number of users receiving a signal level from the nearest HAP below the threshold due to the rainfall. It can be expressed as [1]follows:

$$P = a_{\text{const}} \cdot \left(1 - \left(\frac{\vartheta - \pi}{\pi - b_{\text{const}}\sqrt{1 - (d_{\text{main}}/d_{\text{div}})}}\right)^2\right) \cdot \left(\frac{d_{\text{main}}}{d_{\text{div}}}\right)^{c_{\text{const}}}, \quad (1)$$

where ϑ (rad) and $d_{\text{main}}/d_{\text{div}}$ (–) stand for the angle separation and the ratio of the main and diverse link lengths, respectively. a_{const}, b_{const}, and c_{const} are empirical parameters, that were derived [1] to be dependent on maximum rain rate, the rain fade margin, and the rain spatial parameter (useful for rain spatial classification according to rain impact on system performance).

The results of the analyses of HAP system performance were compared to the outage improvement probability statistics valid for a terrestrial system with the same parameters [25]: transmitter power 30 dBm, HAP antenna gain 29 dBi, ground terminal station antenna gain 39 dBi, and rain margin 24 dB. The particular example of the comparison of outage improvement probabilities as a function of the link length ratio ($d_{\text{main}}/d_{\text{diversity}}$) and the angular separation (φ) is for the particular rain scan as shown in Figure 8. For the sake of clarity, specific values from Figure 8 are given in Table 2.

It can be concluded that when route diversity is utilized a better performance improvement can be observed during a rain event in the HAP network than in the case of a terrestrial point-to-multipoint system. In our example, over 2.6% of mean outage improvement probability can be obtained (up to a peak of 5.5%; for angular separation φ near 180 degrees and a main to diverse link length ratio $d_{\text{main}}/d_{\text{diversity}} = 1/2$).

5. CONCLUSION

In this paper, propagation issues related to HAP systems working at 48 GHz were presented and their specific features were analyzed. A Fabry-Perot resonator-based measurement system was introduced, and simulation and measurement results were discussed. This method can be used to study additional gas attenuation for specific HAP to ground links and inter HAP connections in higher layers of the earth's atmosphere.

The rain attenuation was also analyzed taking into account single link availability as well as the system performance for more complex HAP scenarios. Simulations of HAP system performance using route diversity during a rain event indicated that a higher outage improvement probability can be reached in a HAP system, when compared to a terrestrial point-to-multipoint system.

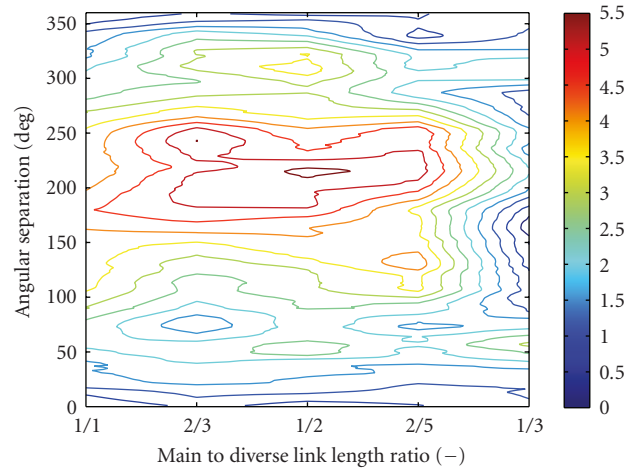

Figure 8: Comparison of outage improvement probabilities for HAP and a terrestrial network for the rain scan from Figure 5.

Table 2: Specific differences between outage improvement probabilities Δ(%)from Figure 8.

Link length ratio (–)	Angular separation (deg)	Δ(%)
1/1	90	3.0
2/3	90	1.8
2/3	180	4.9
1/2	45	2.3
1/2	90	2.6
1/2	180	5.0

ACKNOWLEDGMENTS

The research is a part of the activities of the Department of Electromagnetic Field of the Czech Technical University in Prague within the framework of the research Project of the Ministry of Education, Youth, and Sports of the Czech Republic no. LC06071 Centre of Quasi-Optical Systems and Terahertz Spectroscopy.

REFERENCES

[1] S. Zvanovec and P. Pechac, "Rain spatial classification for availability studies of point-to-multipoint systems," *IEEE Transactions on Antennas and Propagation*, vol. 54, no. 12, pp. 3789–3796, 2006.

[2] J. H. van Vleck, "The absorption of microwaves by oxygen," *Physical Review*, vol. 71, no. 7, pp. 413–424, 1947.

[3] J. H. van Vleck, "The absorption of microwaves by uncondensed water vapor," *Physical Review*, vol. 71, no. 7, pp. 425–433, 1947.
[4] H. J. Liebe, G. G. Gimmestad, and J. D. Hopponen, "Atmospheric oxygen microwave spectrum—experiment versus theory," *IEEE Transactions on Antennas and Propagation*, vol. 25, no. 3, pp. 327–335, 1977.
[5] H. J. Liebe, "Modeling attenuation and phase of radio waves in air at frequencies below 1000 GHz," *Radio Science*, vol. 16, no. 6, pp. 1183–1199, 1981.
[6] International Telecommunications Union, "Attenuation by Atmospheric Gases," ITU-R Recommendation, pp. 676-6, 2005.
[7] E. Salonen, S. Karhu, P. Jokela, et al., "Study of Propagation Phenomena for Low Availability," Final Report, ESA/ESTEC Contract 9455/91/NL/LC(SC), 1994.
[8] P. Kania, L. Stříteská, M. Šimečková, and Š. Urban, "Pressure shifts of acetonitrile ground state parameters," *Journal of Molecular Structure*, vol. 795, no. 1–3, pp. 209–218, 2006.
[9] E. P. Valkenburg and V. E. Derr, "A high-Q Fabry-Perot interferometer for water vapor absorption measurements in the 100 Gc/s to 300 Gc/s frequency range," *Proceedings of the IEEE*, vol. 54, no. 4, pp. 493–498, 1966.
[10] "The FEKO," http://www.feko.info/.
[11] "The CST," http://www.cst.com/.
[12] T. A. Milligan, *Modern Antenna Design*, Wiley-IEEE Press, New York, NY, USA, 2nd edition, 2005.
[13] International Telecommunications Union, "Preferred Characteristics of Systems in the Fixed Service Using High Altitude Platforms Operating in the Bands 47.2–47.5 GHz and 47.9–48.2 GHz," ITU-R Recommendation F.1500, 2000.
[14] S. N. Ghosh and H. D. Edward, "Report No. 82," Geo-Physics Research Directorate, Airforce Cambridge Research Centre, 1956.
[15] Z. Sokol, "The use of radar and gauge measurements to estimate areal precipitation for several Czech River Basins," *Studia Geophysica et Geodaetica*, vol. 47, no. 3, pp. 587–604, 2003.
[16] P. Novak and J. Kracmar, "New data processing in the Czech weather radar network," in *Proceedings of the 2nd European Conference on Radar in Meteorology (ERAD '02)*, vol. 1 of *ERAD Publication Series*, pp. 328–330, Delft, The Netherlands, November 2002.
[17] L. Féral, H. Sauvageot, L. Castanet, and J. Lemorton, "HYCELL—a new hybrid model of the rain horizontal distribution for propagation studies: 1. Modeling of the rain cell," *Radio Science*, vol. 38, no. 3, 2003.
[18] A. Maurolagoitia, J. M. Riera, P. Garcia, and A. Benarroch, "Performance of fade mitigation techniques in a fixed 48 GHz HAPS network," *International Journal of Wireless Information Networks*, vol. 13, no. 1, pp. 19–30, 2006.
[19] COST 255, "Radiowave Propagation Modelling for New Satellite Communication Services at Ku-Band and above," Final Report, Brussels, Belgium, 2002.
[20] K. S. Paulson, R. J. Watson, and I. S. Usman, "Diversity improvement estimation from rain radar databases using maximum likelihood estimation," *IEEE Transactions on Antennas and Propagation*, vol. 54, no. 1, pp. 168–174, 2006.
[21] K. S. Paulson, "Prediction of diversity statistics on terrestrial microwave links," *Radio Science*, vol. 38, no. 3, 2003.
[22] T. Konefal, C. Spillard, and D. Grace, "Site diversity for high-altitude platforms: a method for the prediction of joint site attenuation statistics," *IEE Proceedings: Microwaves, Antennas and Propagation*, vol. 149, no. 2, pp. 124–128, 2002.
[23] A. D. Panagopoulos, E. M. Georgiadou, and J. D. Kanellopoulos, "Selection combining site diversity performance in high altitude platform networks," *IEEE Communications Letters*, vol. 11, no. 10, pp. 787–789, 2007.
[24] S. Zvanovec and P. Pechac, "Wave propagation simulations at 48 GHz for HAPs using rainfall radar data," in *Proceedings of the 1st COST 297—High Altitude Platforms for Communications and Other Services Workshop (HAPCOS '06)*, York, UK, October 2006.
[25] FP6—CAPANINA, "Deliverable 14—Mobile Link Propagation Aspects, Channel Model and Impairment Mitigation Techniques," April 2005.